Journal of Sound and Vibration (2000) **231**(4), 1007–1021
doi:10.1006/jsvi.1999.2446, available online at http://www.idealibrary.com on IDEAL®

AN ANALYTICAL STUDY OF INTERIOR NOISE CONTROL USING SEGMENTED PANELS

S. M. HIRSCH† AND J. Q. SUN

Department of Mechanical Engineering, University of Delaware, Newark, DE 19716, *U.S.A.*

AND

MARK R. JOLLY

Lord Corporation, Thomas Lord Research Center, 405 *Gregson Dr., Cary, NC* 25711, *U.S.A.*

(*Received* 9 *October* 1998; *and in final form* 24 *May* 1999)

This paper presents initial analytical studies of a new method for active interior noise control. The method proposes to control the vibration of segmented trim panels in order to reduce interior noise levels. Since trim panels are often made of light-weight and stiff composite materials, this actuation strategy will enable the creation of active trim panels for interior noise control without using heavy duty structural actuators. The segmentation would provide abilities for both structural sound transmission and active noise control. Numerical studies are performed to demonstrate the effectiveness of segmented trim panels as acoustic control sources. Geometrical design considerations are also studied. A comparison of the forces required for suppressing acoustic pressure is made between segmented trim panels and direct actuation on a single-piece trim panel.

1. INTRODUCTION

Research on active techniques for quieting noise in aircraft has been very active in the past decade. Most of the research can be divided into one of two major categories. The first is active noise control (ANC), which uses acoustic sources such as loudspeakers, to generate a secondary sound field which interacts destructively with the undesired, or primary, sound field. The second approach is active structural acoustic control (ASAC). ASAC is implemented by direct actuation on a vibrating boundary of the enclosure, in order to reduce the sound radiated from the structure into the enclosure. Extensive reviews of ANC and ASAC are contained in references [1–7]. Many benefits and drawbacks of ASAC systems for quieting noise in aircraft are presented by Jones *et al.* [8, 9]. They report that ASAC provides effective control of noise radiated from vibrating elastic structures with fewer control actuators than required for comparable performance from an ANC system.

† Current address: The Boeing Company, PO Box 16858, Philadelphia, PA 19142, U.S.A.

One of the main concerns with structural controls is that they may cause fatigue damages to the structure. This issue is particularly sensitive to the aerospace industry. To avoid this problem, researchers have begun to consider placing actutors on non-critical structures such as interior trim panels of an aircraft [10–15]. It appears that there are difficulties in creating effective interior noise control systems by direct actuation of trim panels. The work by Silcox and his associates [15] represents a significant progress in understanding some important issues regarding structural control applied to fuselage trim panels. In particular, they have found that with a small number of actuators, it is very hard to avoid structural control spillover that can cause the overall interior sound pressure level to increase even though the sound pressure levels at error sensors are well reduced. Tran and Mathur found that an ASAC system implemented with piezoelectric actuators bonded to the trim panel was outperformed by both a traditional ASAC system (direct actuation on the vibrating fuselage) and an ANC system using loudspeakers inside the cabin [14].

Others have considered segmentation of the vibrating boundary, either through the use of acoustic sources or structural modifications to convert the panel into stiff and lightweight sub-panels. Mason and his colleagues have proposed placing a loudspeaker directly on the radiating panel to achieve a zero net volume velocity [16, 17]. Koopman, St. Pierre, Sharp, and Chen have studied volume velocity control of sound transmission through composite panels, employing either loudspeakers or segmented trim panels as volume velocity sources [18–20]. Johnson and Elliott have also studied the control of sound radiation with volume velocity cancellation and arrays of discrete actuators [21, 22]. Leishman and Tichy have presented an excellent summary of research efforts in active control of sound transmission through panels, along with a detailed theoretical analysis of the mechanisms involved [23]. Included in their publication is a proposed actuator configuration which combines boundary segmentation with the addition of a passive diaphragm. It is demonstrated analytically that this double diaphragm should yield very high transmission loss.

In comparison with structural controls on the aircraft skin or frames, actuation of trim panels has several advantages: (1) by moving away from the aircraft skin and frames, safety concerns and the potential cause of fatigue damages to the aircraft structure are eliminated; (2) because trim panels are closer to the acoustic medium and further away from most excitation sources, controlling trim panels may be more effective at reducing cabin noise; (3) trim panels represent a less harsh and steadier environment as compared to the fuselage skin; (4) trim panels are easily retrofittable and replaceable. However, because trim panels are made of lightweight and stiff composites, direct actuation on the panel for noise suppression would likely require very powerful structural control actuators. There is a need to develop advanced actuation technologies for controlling vibration and noise radiation of trim panels. This paper summarizes our recent work on active controls applied to segmented panels for noise suppression. In this study, we apply active controls to segmented panels assuming that each segment of the panel is rigid and is connected to the adjacent segments by an elastometric element with certain damping and stiffness.

Much of the research in the works cited above is focused on active sound transmission control (ASTC). Because of the existence of flanking paths for structural energy transmission in an aircraft, it may not be feasible to control all sound radiated into the cabin through the boundaries. It is important to preserve the ability to actuate directly on the acoustic medium to reduce noise levels due to sound not blocked by structural controls. In this work, we propose the use of segmented trim panels as both ASTC and ANC control sources. Force actuation on trim panel segments can suppress the trim panel vibration in order to reduce the transmitted sound (ASTC). Additionally, the segmented trim panels can be used as effective acoustic sources (ANC). The simulations in this work focus on steady state optimal control studies for minimizing the global interior noise with segmented trim panels as control sources. A simultaneous experimental study, reported elsewhere, has been conducted to verify that segmented trim panels can in fact be used as acoustic sources in an active noise control system [24]. The benefit of the proposed control implementation is that it uses a single set of lightweight, low-profile actuators for a very general control system which efficiently controls all noise in an enclosure, regardless of the source of the noise. The proposed actuation strategy can be implemented by a modification of the trim panel without an extensive installation of additional materials.

The mathematical model for the sound field in a two-dimensional rectangular enclosure is developed in section 2. In section 3, the equations for steady state quadratic optimization corresponding to minimization of total acoustic potential energy are presented. Numerical analysis of the control system is presented in section 4. The mechanisms of acoustic boundary control are studied, as in the control performance of various segmentation configurations. Comparison of control performance and control cost between the segmented rigid beam and a stiff flexible beam is made. The findings of this study are concluded in section 5.

2. THEORETICAL DEVELOPMENT

2.1. ANALYTICAL MODEL

This work utilizes an analytical model of a two-dimensional rectangular enclosure as shown in Figure 1. The two boundaries at $y = 0$ and b are flexible beams. The $x = 0$ boundary is acoustically rigid, while the boundary at $x = a$ is comprised of a segmented rigid beam with N_{seg} segments (Figure 2). Acoustic pressure in the enclosure can be produced by an arbitrary distribution of interior acoustic sources ($Q(x, y, t)$), external forces applied to the two flexible beams ($p_0(x, t)$ and $p_b(x, t)$), and finally by the vibration of the control boundary ($w(y, t)$). Actuators located on the segmented beam are used to alter its vibration to minimize acoustic pressure in the enclosure, effectively using the segmented beam as a distributed acoustic control source. A similar geometrical configuration has been studied by Banks *et al.* [25–27].

The nth segment of the beam at $x = a$ is of length L_n and linear density ρ_n ($n = 1, 2, 3$). The segment joints are elastometric, with effective torsional stiffness and damping, k_i and R_i ($i = 1, 2, 3, 4$). The ends of the segmented beam are attached

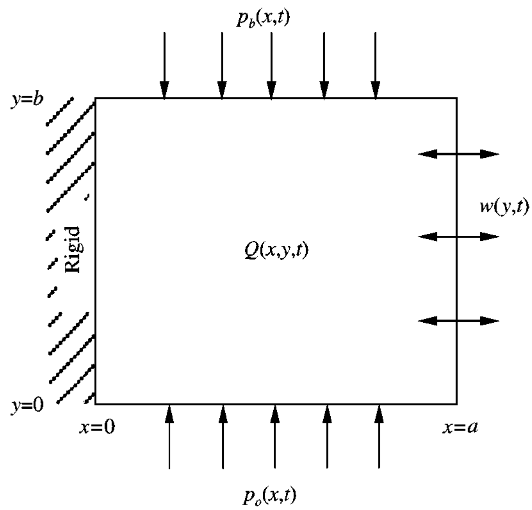

Figure 1. Geometry of a two-dimensional enclosure.

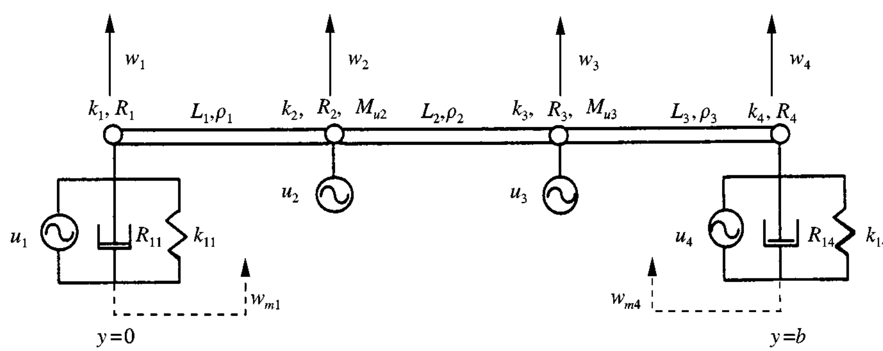

Figure 2. Detailed view of a three-segmented beam.

to elastometric mounts consisting of a linear spring and dashpot ($R_{l1}, R_{l4}, k_{l1}, k_{l4}$). The base of the mounts are in motion described by w_{m1} and w_{m4}. Linear control forces, u_i can be applied at the two mounts; linear control forces and control torques, M_{u2} and M_{u3}, are applied between the segments and referred to as end-mounted actuators. The effect of linear and control torques applied at the center of gravity of each segment is also considered. The beam segments are assumed to be rigid, restricting the system to $N_{\mathrm{d.o.f.}} = N_{seg} + 1$ degrees of freedom. The system can be completely determined by the displacement of the segment endpoints, labelled w_1–w_4.

2.2. STRUCTURAL SOLUTION

Define a displacement vector $\mathbf{w} = [w_1, w_2, \ldots, w_{N_{seg}+1}]^{\mathrm{T}}$. The equations of motion for the beam can be determined with the Lagrangian method, which requires knowledge of the total kinetic and potential energies of the beam, and the virtual work done by the non-conservative forces applied to the beam. Modelling the beam segments as rigid rods, we can express the total kinetic and potential energy of the beam in a compact matrix form,

$$T = \dot{\mathbf{w}}^{\mathrm{T}}(\mathbf{C}_{T\tau} + \mathbf{C}_{Tr})\,\dot{\mathbf{w}}, \tag{1}$$

$$V = \mathbf{w}^{\mathrm{T}}(\mathbf{C}_{V\tau} + \mathbf{C}_{Vr})\mathbf{w} + \tfrac{1}{2}\,k_{l1}(w_{m1}^2 - 2w_1 w_{m1}) + \tfrac{1}{2}\,k_{lN_{d.o.f.}}(w_{mN_{d.o.f.}}^2 - 2w_{N_{d.o.f.}} w_{mN_{d.o.f.}}). \tag{2}$$

The four $\mathbf{C}$ matrices include the contributions from translational and rotation motions (subscripts τ and r) to the kinetic and potential energies (subscripts T and V). The last two terms of equation (2) include the potential energy contribution from the mount excitation of the beam endpoints. The dot notation indicates differentiation with respect to time.

The virtual work done by the non-conservative and applied forces $\mathbf{q}$ can be written as

$$\delta W = \mathbf{q}^{\mathrm{T}}\,\delta\mathbf{w}, \tag{3}$$

where $\delta\mathbf{w}$ is the virtual displacement of $\mathbf{w}$. The force inputs of N_{act} control actuators are combined into an $N_{act} \times 1$ control vector, $\mathbf{u}$. Introduce a control force coupling matrix $\mathbf{U}$ such that the virtual work done by the control forces is

$$\delta W_c = (\mathbf{U}\mathbf{u})^{\mathrm{T}}\,\delta\mathbf{w}. \tag{4}$$

$N_{d.o.f.} \times N_{act}$ control matrix $\mathbf{U}$ couples the motion of these actuators to the motion of the segment endpoints, $\mathbf{w}$. Likewise, define the non-conservative force matrix $\mathbf{F}$ and the mount displacement vector $\mathbf{w}_m = [w_{m1}, w_{mN_{d.o.f.}}]^{\mathrm{T}}$. Express the virtual work done by the non-conservative forces as

$$\delta W_n = (\mathbf{F}\dot{\mathbf{w}}_m)^{\mathrm{T}}\,\delta\mathbf{w}. \tag{5}$$

Therefore, the resultant generalized force vector is given by

$$\mathbf{q} = \mathbf{U}\mathbf{u} + \mathbf{F}\dot{\mathbf{w}}_m. \tag{6}$$

Applying Lagrange's equations for finite degree-of-freedom systems, we obtain the equations of motion for the segmented beam:

$$\mathbf{M}\ddot{\mathbf{w}} + \mathbf{R}\dot{\mathbf{w}} + \mathbf{K}\mathbf{w} = \mathbf{U}\mathbf{u} + \mathbf{f}, \tag{7}$$

where M, $\mathbf{R}$, $\mathbf{K}$, and $\mathbf{f} = \mathbf{F}\dot{\mathbf{w}}_m$ are the mass, damping, and stiffness matrices and the force vector respectively.

For harmonic response at angular frequency ω, we obtain

$$\mathbf{w} = \mathbf{D}^{-1}(\mathbf{U}\mathbf{u} + \mathbf{f}), \tag{8}$$

where the dynamic matrix $\mathbf{D} = -\omega^2\mathbf{M} + \mathrm{j}\omega\mathbf{R} + \mathbf{K}$. The continuous solution for beam displacement can be constructed from the motion of the segment endpoints:

$$w(y,t) = \begin{cases} w_1 + \left(\dfrac{w_2 - w_1}{l_1}\right), & 0 \leqslant y \leqslant l_1, \\ w_2 + \left(\dfrac{w_3 - w_2}{l_2}\right)(y - l_1), & l_1 \leqslant y \leqslant (l_1 + l_2), \\ \vdots & \\ w_{N_{seg}} + \left(\dfrac{w_{N_{seg}+1} - w_{N_{seg}}}{l_{N_{seg}}}\right)\left(y - \sum\limits_{n=1}^{N_{seg}-1} l_n\right), & \sum\limits_{n=1}^{N_{seg}-1} l_n \leqslant y \leqslant b \end{cases}. \tag{9}$$

Recall that the beam serves as one boundary of the acoustic enclosure. Continuity requires that the velocity of the acoustic media match the velocity of the structure at this boundary ($x = a$). In anticipation of a modal solution for the acoustic velocity with cosine eigenfunctions, we expand the beam displacement as an infinite cosine series:

$$w(y,t) = \sum_{n=0}^{\infty} W_n(t)\cos\frac{n\pi y}{b}, \quad W_n(t) = \mathbf{e}_n^{\mathrm{T}}\mathbf{w}(t), \tag{10}$$

where the $N_{d.o.f.} \times 1$ column vector $\mathbf{e}_n$ is defined such that

$$\mathbf{e}_n^{\mathrm{T}}\mathbf{w}(t) = \begin{cases} \dfrac{2}{b}\displaystyle\int_0^b w(y,t)\cos\frac{n\pi y}{b}\,\mathrm{d}y, & n > 0, \\ \dfrac{1}{b}\displaystyle\int_0^b w(y,t)\,\mathrm{d}y, & n = 0. \end{cases} \tag{11}$$

2.3. ACOUSTIC SOLUTION

Under the assumption of Euler's equation, one form of the Kirchhoff–Helmholtz integral equation for pressure in an enclosure at angular frequency ω is [28]

$$p(\mathbf{r},\omega) = \int_S \left[p(\mathbf{r}_s)\frac{\partial G}{\partial n}(\mathbf{r}|\mathbf{r}_s) + \mathrm{j}\omega\rho_0\dot{w}(\mathbf{r}_s)\,G(\mathbf{r}|\mathbf{r}_s)\right]\mathrm{d}S + \mathrm{j}\omega\rho_0\int_V Q(\mathbf{r}_0)\,G(\mathbf{r}|\mathbf{r}_0)\,\mathrm{d}V, \tag{12}$$

where surface, interior source, and observation locations are indicated by $\mathbf{r}_s$, $\mathbf{r}_0$, and $\mathbf{r}$, respectively, n denotes the normal of the surface S, and G is the enclosure Green's function. $\dot{w}(\mathbf{r}_s)$ is the outward normal velocity of the surface at $\mathbf{r}_s$ and $Q(\mathbf{r}_0)$ is the volume velocity of an acoustic source at $\mathbf{r}_0$. Inherent in this equation is a continuity between the velocity of vibrating boundaries and the acoustic media. The first integral of equation (12) is computed over all boundaries of the enclosure. The second integral is evaluated over the entire interior and includes the contribution due to source inside the enclosure. The enclosure Green's function can be approximated by a series of the acoustic mode functions for the rigid-walled enclosure. For a two-dimensional rectangular enclosure,

$$G(\mathbf{r}|\mathbf{r}_0) = \sum_{\hat{m}=0}^{\infty} \sum_{\hat{n}=0}^{\infty} \frac{\phi_{\hat{m}\hat{n}}(\mathbf{r}_0)}{k_{\hat{m}\hat{n}}^2 - k^2} \phi_{\hat{m}\hat{n}}(\mathbf{r}), \tag{13}$$

$$\phi_{\hat{m}\hat{n}} = \varepsilon_{\hat{m}\hat{n}} \cos\left(\frac{\hat{m}\pi x}{a}\right) \cos\left(\frac{\hat{n}\pi y}{b}\right), \quad \hat{m}, \hat{n} = 0, 1, 2, \ldots . \tag{14}$$

$$\varepsilon_{\hat{m}\hat{n}} = \varepsilon_{\hat{m}} \varepsilon_{\hat{n}}, \quad \varepsilon_{\hat{m}} = \begin{cases} \sqrt{\dfrac{1}{a}}, & \hat{m} = 0, \\ \sqrt{\dfrac{2}{a}}, & \hat{m} > 0, \end{cases} \quad \varepsilon_{\hat{n}} = \begin{cases} \sqrt{\dfrac{1}{b}}, & \hat{n} = 0, \\ \sqrt{\dfrac{2}{b}}, & \hat{n} > 0, \end{cases} \tag{15}$$

where $\phi_{\hat{m}\hat{n}}(\mathbf{r})$ is a set of orthogonal eigenfunction satisfying the homogeneous Helmholtz equation and the rigid-wall boundary condition, with eigenvalues $k_{\hat{m}\hat{n}}^2 = (\hat{m}\pi/a)^2 + (\hat{n}\pi/b)^2$. Energy losses of the enclosure are included via a complex eigenvalue, $k_{\hat{m}\hat{n}} = k_{\hat{m}\hat{n}}(1 + \mathrm{j}\zeta)$, where ζ is a very small loss factor. The acoustic wave number is $k = \omega/c$, c is the speed of sound in the air. By construction, the first term of the first integral of equation (12) is zero. The choice of a rigid-walled boundary condition seems contradictory with the inclusion of vibrating boundaries. This formulation for acoustic pressure in an enclosure can be viewed as utilizing a superposition of the sound field in a rigid-walled enclosure with the acoustic pressure radiated from its vibrating boundaries. Jayachandran *et al.* [29] have demonstrated that this solution is very accurate inside the enclosure, gives an extremely accurate mean square measure, but is inaccurate at the vibrating boundaries.

Assume that the series for Green's function are truncated to contain the first $\hat{M} + 1$ and $\hat{N} + 1$ terms. Then, the Kirchhoff–Helmholtz integral equation can be written as

$$p(\mathbf{r}, \omega) = (\mathbf{Q}(\omega) - \mathbf{V}(\omega) - \mathbf{T}(\omega))^{\mathrm{T}} \phi(\mathbf{r}), \tag{16}$$

where $\phi = [\phi_{00}, \phi_{01}, \ldots, \phi_{\hat{M}\hat{N}}]^{\mathrm{T}}$ is the modal function vector. The elements of column vectors **Q**, **V**, and **T** represent modal contributions of the interior source, side-structural vibration and the control input from the segmented beam respectively. Computation of **Q** and **V** can be found in references [6, 28]. The modal elements of matrix **T** can be obtained as follows:

$$T_{\hat{m}\hat{n}} = \frac{\mathrm{j}\omega\rho}{k_{\hat{m}\hat{n}}^2 - k^2} \int_0^b \dot{w}(y) \phi_{\hat{m}\hat{n}}(y) \, \mathrm{d}y = (-1)^{\hat{m}+1} \frac{\omega^2 \rho}{k_{\hat{m}\hat{n}}^2 - k^2} \frac{\varepsilon_{\hat{m}}}{\varepsilon_{\hat{n}}} W_{\hat{n}} \tag{17}$$

$$= (-1)^{\hat{m}+1} \frac{\omega^2 \rho}{k_{\hat{m}\hat{n}}^2 - k^2} \frac{\varepsilon_{\hat{m}}}{\varepsilon_{\hat{n}}} \mathbf{e}_{\hat{n}}^{\mathrm{T}} \mathbf{w} = (-1)^{\hat{m}+1} \frac{\omega^2 \rho}{k_{\hat{m}\hat{n}}^2 - k^2} \frac{\varepsilon_{\hat{m}}}{\varepsilon_{\hat{n}}} \mathbf{e}_{\hat{n}}^{\mathrm{T}} \mathbf{D}^{-1} (\mathbf{U}\mathbf{u} + \mathbf{f}) = \mathbf{b}_{\hat{m}\hat{n}} \mathbf{u} + T_{\hat{m}\hat{n}}^{f}, \tag{18}$$

where

$$\mathbf{b}_{\hat{m}\hat{n}} = (-1)^{\hat{m}+1} \frac{\omega^2 \rho}{k_{\hat{m}\hat{n}}^2 - k^2} \frac{\varepsilon_{\hat{m}}}{\varepsilon_{\hat{n}}} \mathbf{e}_{\hat{n}}^{\mathrm{T}} \mathbf{D}^{-1} \mathbf{U}, \tag{19}$$

$$T_{\hat{m}\hat{n}}^{f} = (-1)^{\hat{m}+1} \frac{\omega^2 \rho}{k_{\hat{m}\hat{n}}^2 - k^2} \frac{\varepsilon_{\hat{m}}}{\varepsilon_{\hat{n}}} \mathbf{e}_{\hat{n}}^{\mathrm{T}} \mathbf{D}^{-1} \mathbf{f}. \tag{20}$$

$\mathbf{b}_{\hat{m}\hat{n}}$ is a row vector of length N_{act} which couples the control force to the response of the $\hat{m}\hat{n}$th acoustic mode and $T_{\hat{m}\hat{n}}^{f}$ is scalar denoting the acoustic response to undesired vibration of the segmented boundary excited by the mount base movement. Orthogonality of the eigenfunctions yields $T_{\hat{m}\hat{n}} = 0$ for $\hat{n} \neq n$, hence $W_n = W_{\hat{n}}$ and $\mathbf{e}_n = \mathbf{e}_{\hat{n}}$.

3. OPTIMAL CONTROL

The goal of an interior acoustic control system is to achieve global noise reduction in an enclosure. In this work, the cost function for the optimal control system is total acoustic potential energy. The cost function can be expressed in the standard Hermitian quadratic form

$$J = \int_V p^*(\mathbf{r}) p(\mathbf{r}) \, \mathrm{d}V \tag{21}$$

$$= \mathbf{u}^H \mathbf{A} \mathbf{u} + \mathbf{u}^H \mathbf{a} + \mathbf{a}^H \mathbf{u} + J_0, \tag{22}$$

$$\mathbf{A} = \mathbf{B}^H \mathbf{B}, \qquad \mathbf{a} = \mathbf{B}^H (\mathbf{Q} - \mathbf{V}), \qquad J_0 = (\mathbf{Q} - \mathbf{V})^H (\mathbf{Q} - \mathbf{V}), \tag{23–25}$$

where $\mathbf{B} = [\mathbf{b}_{00}^{\mathrm{T}}, \mathbf{b}_{01}^{\mathrm{T}}, \ldots, \mathbf{b}_{\hat{M}\hat{N}}^{\mathrm{T}}]^{\mathrm{T}}$. $\mathbf{A} = \mathbf{A}^H$ is a positive-definite $N_{act} \times N_{act}$ matrix, $\mathbf{a}$ is an $N_{act} \times 1$ complex vector, and J_0 is a real scalar which indicates the value of the cost function without influence of the controller. Superscript ^{H} denotes the Hermitian transpose. Note that J is real and positive by construction. Dependence of all terms on frequency is suppressed for compactness of notation.

The optimal control solution is found by minimizing J with respect to the control vector:

$$\frac{\mathrm{d}J(\mathbf{u})}{\mathrm{d}\mathbf{u}} = \mathbf{0}, \qquad \mathbf{u}_{opt} = -\mathbf{A}^{-1} \mathbf{a}. \tag{26, 27}$$

4. NUMERICAL RESULTS

Numerical studies are conducted of the system represented in Figure 1. The primary goal of these studies is to determine the effectiveness of the segmented control boundary in cancelling noise in the enclosure. Additionally, we study the effects of the number and size of the beam segments on control performance. The effect of actuator placement on the control cost is studied. Finally, comparisons of control performance and cost are made between the segmented beam and a continuous beam made of the trim panel material. This comparison is made to determine if the segmentation procedure provides advantages over direct actuation on the trim panel.

The enclosure is of dimension $1{\cdot}2 \times 1{\cdot}1\ \mathrm{m}^2$. The boundaries at $y = 0$, b are modelled as 5 mm thick simply supported aluminium beams. The segmented beam has a density of $335\ \mathrm{kg/m^3}$, thickness of 6·3 mm, and unit width. The elastometric joints of the segmented control beam have a rotational stiffness of 549·5 N/m and a rotational damping of 0·63 N s/m. These are typical values for the suspension of a loudspeaker. The joint stiffness and damping could also be implemented as tunable devices, leading to an adaptive-passive segmented trim panel. An acoustic source of volume velocity $0{\cdot}008\ \mathrm{m^3/s}$ is located at $(\hat{x}_0, \hat{y}_0) = 0{\cdot}01\ (a, b)$ and a 1000 N point force is placed at $x_0 = 0{\cdot}01a$ on the $y = 0$ boundary.

4.1. CONTROL EFFECTIVENESS OF SEGMENTED BEAM

Figure 3 demonstrates that the segmented beam is an effective acoustic control source. The mean pressure in the enclosure is plotted as function of frequency both before and after control is applied. The control panel is comprised of five segments. Pressure levels are reduced at all frequencies in the presented range. The average reduction is 9·1 dB over the frequency range shown. The attenuation of mean pressure is smallest near resonance frequencies of the side walls which lie a reasonable distance from any natural frequencies of the enclosure. When excited between acoustic resonances, the sound field contains contributions from many acoustic modes, making it more difficult for the control source to accurately produce the cancellation sound field [30].

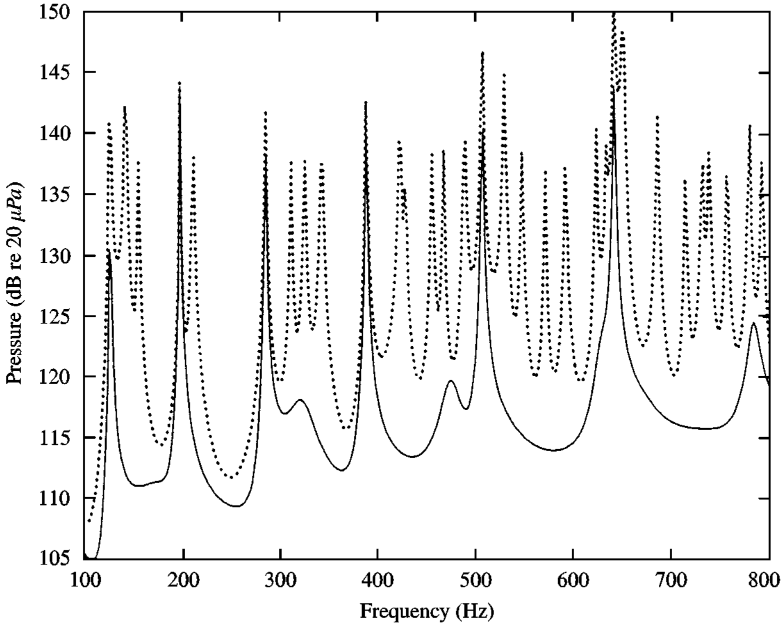

Figure 3. Mean pressure in two-dimensional enclosure: . . . . . ., the uncontrolled sound field due to an acoustic source of volume velocity $0{\cdot}008\ \mathrm{m^3/s}$ located at $(\hat{x}_0, \hat{y}_0) = 0{\cdot}01\ (a, b)$ and a 1000 N point force placed at $x_0 = 0{\cdot}01a$ on the $y = 0$ boundary; ——, after control with five-segment control beam.

4.2. CONTROL PANEL GEOMETRY

The effect of the number of segments on control performance is shown in Figure 4. It is observed that increasing the number of segments increases the upper frequency to which the beam is an effective control source. This results from the increased number of degrees of freedom of the beam with more segments. Figure 5 presents a comparison of the effect of segment lengths on control performance. These results suggest that segment length is not a major consideration.

The dependence of control cost on actuator placement along the segmented beam shown in Figure 6. Three configurations of four actuators on a three-segment beam are considered: (1) u_1–u_4; (2) u_2, u_3, M_{u2}, and M_{u3}; and (3) one linear and one torque actuator at the center of gravity of the outer segments. It is observed that the optimal control force can be significantly lower for center-mounted actuators than for end-mounted actuators. Since these actuator configurations each provide complete controllability of the segmented beam, they provide identical control performance.

When comparing the control effort, we have only used the norm of the optimal control vector. It should be noted that whenever both linear force actuators and torque actuators are involved in the comparison, one should use a common basis for comparison such as electric power consumption of the actuator. However, we have not addressed the issue at this level.

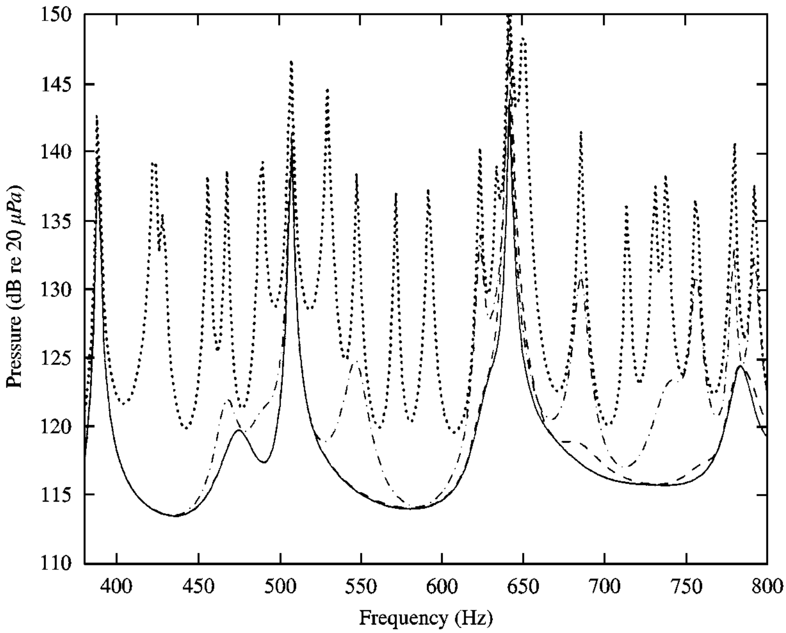

Figure 4. Mean pressure in two-dimensional enclosure, comparing the control effectiveness of beams comprised of a various number of segments. Mean pressure in two-dimensional enclosure: . . . . ., the primary sound field due to an acoustic source of volume velocity 0·008 m^3/s located at $(\hat{x}_0, \hat{y}_0) = 0{\cdot}01\ (a, b)$ and a 1000 N point force placed at $x_0 = 0{\cdot}01a$ on the $y = 0$ boundary; — · — · —, after control with two segment control beam; – – –, after control with three-segment control beam; ——, after control with five-segment control beam.

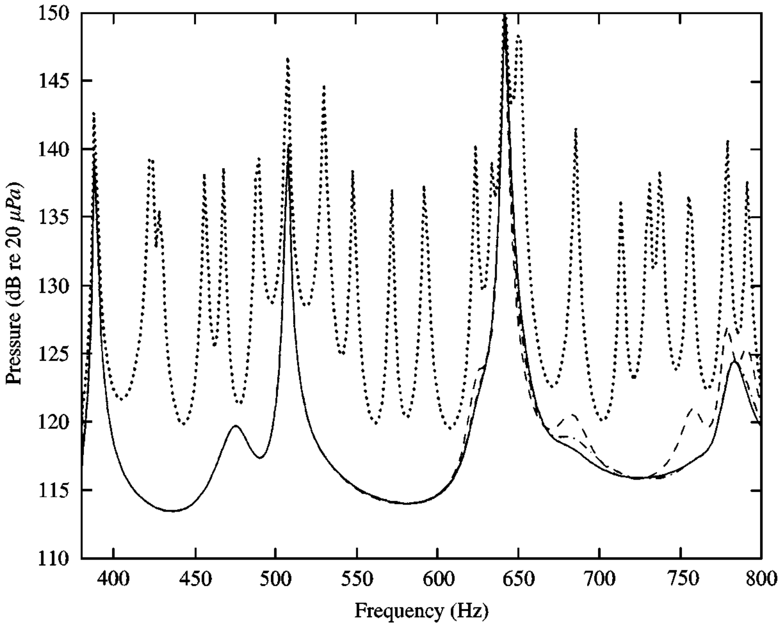

Figure 5. Mean measure in two-dimensional enclosure comparing the control effectiveness for various segment sizes of a three-segment beam: . . . . . , the primary sound field due to an acoustic source of volume velocity 0·008 m^3/s located at $(\hat{x}_0, \hat{y}_0) = 0{\cdot}01\,(a, b)$ and a 1000 N point force placed at $x_0 = 0{\cdot}01a$ on the $y = 0$ boundary; — · — · —, and ——, after control with segment sizes of [0·3, 0·5, 0·2], [0·28, 0·4, 0·32], and [0·2, 0·6, 0·2], respectively.

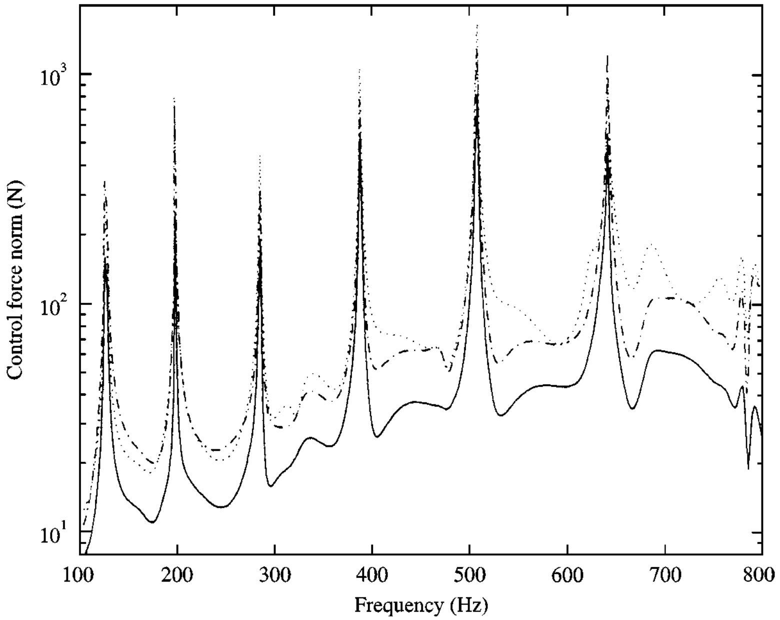

Figure 6. Comparison of control effort for various actuator configurations on a three-segment beam. The primary sound field is due to an acoustic source of volume velocity 0·008 m^3/s located at $(\hat{x}_0, \hat{y}_0) = 0{\cdot}01\,(a, b)$ and a 1000 N point force placed at $x_0 = 0{\cdot}01a$ on the $y = 0$ boundary: . . . . . , one linear actuator at each segment end; – · – · –, one linear and one torsional actuator at each inner segment joint; ——, one linear and one torsional actuator at the center of each outer segment.

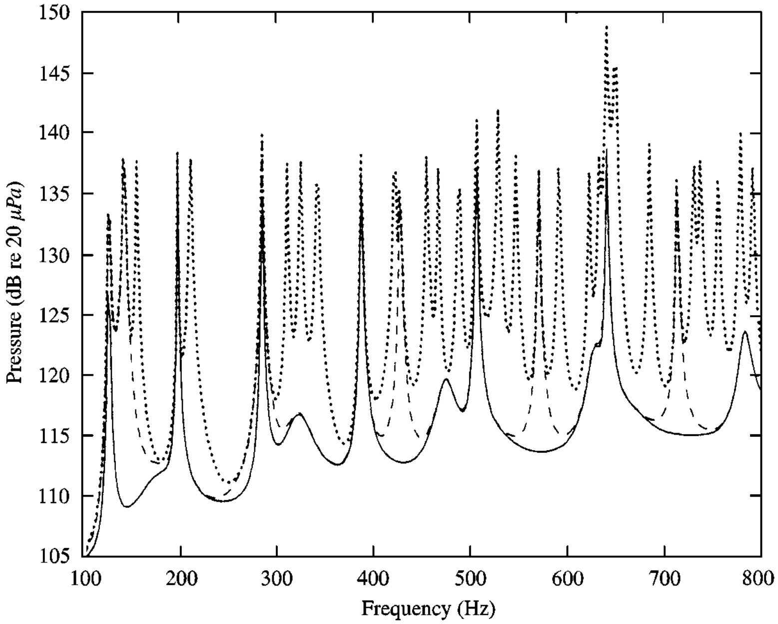

Figure 7. Mean pressure in two-dimensional enclosure comparing the control effectiveness of a rigid segmented beam and a flexible composite beam: . . . . . , the primary sound field due to an acoustic source of volume velocity 0·008 m^3/s located at $(\hat{x}_0, \hat{y}_0) = 0{\cdot}01\ (a, b)$ and a 1000 N point force placed at $x_0 = 0{\cdot}01a$ on the $y = 0$ boundary; — ——, and ——, after control with flexible and segmented beams respectively.

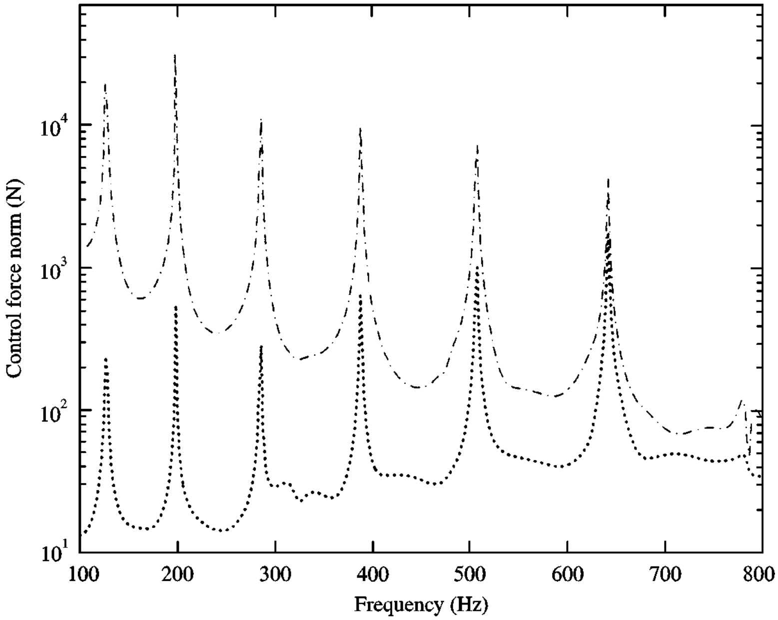

Figure 8. Comparison of control effort for a rigid segmented beam and a flexible composite beam. The primary sound field is due to an acoustic source of volume velocity 0·008 m^3/s located at $(\hat{x}_0, \hat{y}_0) = 0{\cdot}01\ (a, b)$ and a 1000 N point force placed at $x_0 = 0{\cdot}01a$ on the $y = 0$ boundary: – · – · –, continuous composite beam with six actuators; ——, five-segment beam.

4.3. COMPARISON OF SEGMENTED-BEAM WITH COMPOSITE BEAM

The control studies are repeated with an elastic composite beam replacing the segmented control beam. The density, width, and thickness are the same as the segmented beam material. The Young's modulus is $8{\cdot}25 \times 10^{10}$. These material properties are the same as those of a typical trim panel for business jets. It is observed that an elastic beam with six linear force actuators placed at the nodes of its seventh mode provides nearly the same control performance to a five-segment beam through 800 Hz as shown in Figure 7. The control cost of the elastic beam is compared with that of the five-segment beam in Figure 8. The segmented beam is controlled by one linear and one torque actuator at the center of the first, third, and fifth segments, for a total of six actuators. The control cost is lower for the segmented beam over the entire frequency range presented. The advantage is greatest at low frequencies. It is noted that the control cost for the elastic beam would be significantly lower for materials such as aluminium. Recall that the purpose of this study is to design a control source for ANC and ASTC systems which involves primarily a modification of structures such as trim panels already in aircraft.

5. CONCLUSION

A mathematical model of an enclosure with a flexible side made of a segmented rigid beam has been developed. The segmented beam allows low power structural actuation for interior noise control. Some issues of the segmented beam geometry and actuator placement are studied. The numerical results suggest that, while the relative length of individual beam segments does not greatly affect control performance, the number of beam segments does. Increasing the number of segments (and hence, the number of degrees of freedom of the beam system) increases the upper frequency to which the acoustics pressure can be controlled. Comparisons of this control strategy with the approach of direct actuation on a stiff, elastic beam suggest that, given the same number of control actuators, the segmented beam provides nearly the same control performance with lower applied force.

ACKNOWLEDGMENT

This work is supported in part by a grant (CMS-9634672) from the National Science Foundation, and a grant from the State of Delaware Research Partnership program and Lord Corporation. Support by the Delaware Space Grant College Fellowship Program for S. M. Hirsch during the course of this work is also gratefully acknowledged.

REFERENCES

1. D. C. SWANSON, 1989 *ASHRAE Transactions*, **95**, 63–76. Active attenuation of acoustic noise: past, present and future.
2. K. K. AHUJA and J. C. STEVENS 1990 *AIAA Journal* **29**, 1058–1067. Recent advances in active noise control.

3. G. Miccoli and A. Concilio 1994 *Proceedings of the Third International Congress on Air- and Structure-borne Sound and Vibration*, Vol. 3, 1377–1384. Montreal, Canada. Recent advances in noise and vibration active control by means of piezoelectric transducers.
4. C. Ross 1989 *Noise Vibration Control Worldwide*, **20**, 171–173. Current developments and future trends in active noise control.
5. J. Tichy 1991 *Journal of the Acoustical Society of Japan* (*E*) **12**, 255–262. Current and future issues of active noise control.
6. P. A. Nelson and S. J. Elliot 1992 *Active Control of Sound*. New York: Academic Press.
7. C. R. Fuller, S. J. Elliott and P. A. Nelson 1996 *Active Control of Vibration*. San Diego, CA. Academic Press.
8. J. D. Jones and C. R. Fuller 1990 *The International Journal of Analytical and Experimental Modal Analysis* **5**, 123–140. Active control of structurally-coupled sound fields in elastic cylinders by vibrational force inputs.
9. C. R. Fuller and R. J. Silcox 1992 *Journal of the Acoustical Society of America* **91**, 519. Active structural acoustic control.
10. F.W. Grosveld, T. J. Coats, H. C. Lester and R. J. Silcox 1994 *Proceedings of the National Conference on Noise Control Engineering*, 403–408. Fort Lauderdale, FL. Numerical study of active structural acoustic control in a stiffened, double wall cylinder.
11. K. H. Lyle and R. J. Silcox 1995 *Aerospace Engineering* (*Warrendale*, *Pennsylvania*) **15**, 21–25. Active trim panels for aircraft interior noise reduction.
12. K. H. Lyle and R. J. Silcox 1996 *S.A.E. Transactions* **104**, 180. A study of active trim panels for interior noise reduction in an aircraft fuselage.
13. D. R. Thomas, P. A. Nelson, S. J. Elliott and R. J. Pinnington 1993 *Noise Control Engineering* **41**, 273–279. An experimental investigation into the active control of sound transmission through stiff light composite panels.
14. B. N. Tran and G. P. Mathur 1996 *Proceedings of the* 1996 *National Conference on Noise Control Engineering. Part* 1 (*of* 2), 395–400. Bullevue, Washington. Aircraft interior noise reduction tests using active trim panels.
15. R. J. Silcox, K. H. Lyle, V. L. Metcalf and D. E. Brown 1995 *Proceedings of the First Joint CEAS/AIAA Aeronautics Conference*, Vol. II, 1095–1104. Munich, Germany. A study of active structural acoustic control applied to the trim panels of a large scale fuselage model.
16. B. V. Mason, K. Naghshineh and G. K. Toth 1994 *Proceedings of Noise Conference* 467–472. Brodband, wide-area active control of sound radiation from vibrating structures using local surface-mounted radiation suppression devices.
17. B. V. Mason, G. K. Toth, K. Naghshineh and J. W. Kamman 1995 *Proceedings of ASME Winter Annual Meeting*, 95–WA/NCA–8. San Francisco, CA. A feedforward controller for active reduction of radiated noise from a uniformly vibrating circular plate.
18. R. L. St. Pierre Jr., W. Chen and G. H. Koopmann 1995 *Proceedings of ASME Winter Annual Meeting*. San Francisco, CA. Design of adaptive panels with high transmission loss characteristics.
19. R. L. St. Pierre Jr., G. H. Koopmann and W. Chen 1997 *Journal of Sound and Vibration* **210**, 441–460. Volume velocity control of sound transmission through composite panels.
20. S. J. Sharp, G. H. Koopman and W. Chen 1997 In *Proceedings of Noise-Conference* 1997, 149–160. Transmission loss characteristics of an active trim panel.
21. M. E. Johnson and S. J. Elliott 1995 *Journal of the Acoustical Society of America* **98**, 2174–2186. Active control of sound radiation using volume velocity cancellation.
22. M. E. Johnson and S. J. Elliott 1997 *Journal of Sound and Vibration* **207**, 743–759. Active control of sound radiation from vibrating surfaces using arrays of discrete actuators.

23. T. W. Leishman and J. Tichy 1997 *Proceedings of Noise-Conference* 1997, 137–148. The Pennsylvania State University. A fundamental investigation of the active control of sound transmission through segmented partition elements.
24. S. M. Hirsch, N. E. Meyer, M. A. Westervelt, P. King, F. J. Li, M. V. Petrova and J. Q. Sun 2000 *Journal of Sound and Vibration* **231**, 1023–1037. Experimental study of smart segmented trim panels for aircraft interior noise control.
25. H. T. Banks and W. Fang 1991 *Proceedings of* 30*th IEEE Conference on Decision and Control*, Vol. 3, 2328–2333. Brighton, England. Active noise control: piezoceramic actuators in fluid/structure interaction models.
26. H. T. Banks, R. J. Silcox and R. C. Smith 1994 *Journal of Vibration and Acoustics* **116**, 386–396. Modeling and control of acoustic structure interaction problems via piezoceramic actuators: 2-d numerical examples.
27. H. T. Banks, R. C. Smith, Y. Wang, D. E. Brown, V. L. Metcalf and R. J. Silcox 1994 *Proceedings of Proceedings of the* 33*rd IEEE Conference on Decision and Control. Part* 1 (*of* 4), 305–310. Lake Buena Vista, FL. Noise control in a 3-d structural acoustic system: numerical and experimental implementation of a pde-based methodology.
28. F. Fahy 1985 *Sound and Structural Vibration—Radiation, Transmission and Response*. New York: Academic Press.
29. V. Jayachandran, S. M. Hirsch and J. Q. Sun 1998 *Journal of Sound and Vibration* **210**, 243–254. On the numerical modeling of interior sound fields by the modal function expansion.
30. S. Laugesen and S. J. Elliott 1993 *IEEE Transactions on Speech and Audio Processing*, **1**, 241–249. Multichannel active control of random noise in a small reverberant room.